High-performance screen-printed Au/Ba0.85Sr0.15TiO3/Pt capacitors for tunable devices

Aymen Selmi, O. Khaldi, Manuel Mascot, F. Jomni, Jean-Claude Carru

High-performance screen-printed Au/$Ba_{0.85}Sr_{0.15}TiO_3$/Pt capacitors for tunable devices

A. Selmi[a, b*], O. Khaldi[a], M. Mascot[b], F. Jomni[a], J-C. Carru[b]

[a] *Laboratory of Materials Organisation and Properties (LR99ES17) Faculty of Sciences of Tunis, University of Tunis El Manar2092, Tunis Tunisia*
[b] *Université du Littoral Côte d'Opale, Unité de Dynamique et Structure des Matériaux Moléculaires, F-62228 Calais, France*

[*] *Corresponding author: E-mail address: eyman_selmi@yahoo.fr , Phone: (+216) 21 061 882*

Abstract

Metal-Ferroelectric-Metal capacitor structure, employing the lead free ferroelectric $Ba_{0.85}Sr_{0.15}TiO_3$ thick films **are** successfully prepared by screen printing process on silicon platinized Pt/Ti/SiO_2/Si substrates. The surface morphology and microstructure **are** analyzed by scanning electron microscope and X-ray diffraction. The thick film showed a well adhesion to the Pt/Ti/SiO_2/Si substrate and uniform thickness of about ~20 µm. The frequency **dependence of** dielectric characteristics of BST thick films **are** systematically discussed and compared in a large temperature range. Ferroelectric characterizations, tunability and leakage current in the Au/BST(thick film)/Pt capacitor were also studied at room temperature by polarization cycles (P-V) , Capacitance (C-V) and current (I-V) measurements. The high tunability (81%) combined with the low dielectric loss **tangent** and low leakage current makes $Ba_{0.85}Sr_{0.15}TiO_3$ thick films one of the encouraging candidates for various modern **electronic** tunable devices.

Key Words: Lead-free BST thick film; Screen printing; Dielectric properties; ac conductivity; Tunability, leakage current

1. Introduction

The demand for tunable ferroelectric components in microelectronic field increased during the last years. Tunable microwave systems such as tunable varactors diodes, tunable oscillators, filters, FeRAM or tunable ferroelectric capacitors are becoming more and more important [1-7]. For this type of application the ferroelectric oxide materials are the most promising candidates. In terms of tunability, Barium Strontium Titanate ($Ba_xSr_{1-x}TiO_3$ or BST) is considered to be the archetype of electrically tunable materials [2, 8]. BST materials are known for their exceptional properties. So, aside from their high tunability and their environment friendly nature, ferroelectric BST can be prepared with high dielectric permittivity, small leakage-current and low dielectric losses [9, 10]. Thanks to all these unique characteristics, BST shows great promise for the conception of microwave tunable devices and are the more most extensively studied material to date because of the demand for lead-free ferroelectric materials [11]. For integration in microelectronic devices, BST has been investigated in various forms, including thin films with a thickness typically less than1µm, thick films with a few micrometers thick and ceramics with millimeter size. During these last years, the majority of the studies on BST were oriented towards the study of thin films and to a lesser extent towards ceramics but there have been few studies published on BST thick. Currently, the thick films of BST have received some attention; several recent research works have mentioned the importance of these materials in various applications of microelectronics [2, 12]. BST Thick films with thickness ranging from1µm to100µm can significantly replace BST ceramics in case of miniaturization and can be useful to fulfill the demands for multilayer assembles and circuit complexity and also can bridge the technological gap between BST ceramics and BST thin films [2]. To prepare BST thick films with a few micrometers thickess, the preferred technique is the screen printing; this technique has received a lot of attention due to its exceptional characteristics including the good quality of the deposited films, the potential benefits of lower fabrication costs compared to other technique and the possibility to use different types of substrates whatever their geometry and morphology [13, 14]. This process depends on two essential parameters, the preparation of BST ink and heat treatments at high temperatures. The major frequent difficulty in depositing BST thick films by screen printing technology is the quality of the adhesion of the film to the substrate; this phase requires good ink quality, well studied thermal treatments and a good choice of substrate. Presently, Alumina Al_2O_3 is the commonly used substrate in the deposition of BST thick films using screen printing process. However, some studies showed that deposited BST films are very reactive with Al_2O_3 substrates during heat treatment at high

temperature [15]; this phenomenon strongly influences the performance of **the** elaborated thick films [16]. To the best of our knowledge, to date the deposition of BST in thick films form by **performed** screen printing process on Pt/Ti/SiO2/Si substrates has not yet been studied despite the technological importance of this type of substrate. **The usage of $Pt/Ti/SiO_2/Si$ substrates is known as for a high temperature stable metallization which withstands high temperatures (up to 750-800°C). In order to ensure good adhesion and low resistivity suitable for depositing ferroelectric oxide thin films, we have used Titanium as an adhesion layer. Then In consequence, the electrical performance of BST thick films on these platinized silicon substrates can could be higher than the ones deposited on alumina substrates.** In this view, we propose a detailed study on elaborations and characterizations of $Ba_{0.85}Sr_{0.15}TiO_3$ thick films on Pt/Ti/SiO2/Si substrates. **The composition BST85/15 is a good trade-off between having very good ferroelectric and dielectric properties for applications at temperatures close to room temperature.** In this work, high-quality $Ba_{0.85}Sr_{0.15}TiO_3$ thick films **of** 20 µm thick are successfully fabricated by screen-printing technique on Pt/Ti/SiO2/Si. Dielectric permittivity, dielectric loss and AC conductivity of $Ba_{0.85}Sr_{0.15}TiO_3$ thick films **are** investigated as a function of temperature, frequency and applied voltage. Ferroelectric properties and tunability were also analyzed using Polarization-Voltage (P-V) and Capacitance-Voltage (C-V) measurements. Moreover, the conduction mechanisms in Au/$Ba_{0.85}Sr_{0.15}TiO_3$/Pt thick capacitors **are investigated** using current-voltage (J-V) measurements. It is shown that our ferroelectric $Ba_{0.85}Sr_{0.15}TiO_3$ thick films present high performance and are therefore encouraging candidates in the areas of thick film technology.

2. Experimental process

2.1 The differents steps of thick films préparation

$Ba_{0.85}Sr_{0.15}TiO_3$ thick layer **is** preparated by employ a screen printing **device** (TIFLEX - HL570S). The powders of BST **are synthesized** by the solid-state procedure from Strontium oxide (SrO) ,Barium oxide (BaO), and Titanium oxide (TiO_2) **from Alfa Aesar(99.5% purity).** The ink for screen printing **is synthesized** by blending BST powders with organic vehicles. The organic vehicles **is** composed of {alpha-terpineol ($C_{10}H_{18}O$) **from Across Organics (97% purity)**, polyvinyl butyral $(C_8H_{14}O_2)n$, **from Across Organics(98% purity),** 2-(2-butoxyethoxy)-ethyl acetate ($C_{10}H_{20}O_4$) **from Sigma Aldrich (99% purity)** and polyethylene glycol (C_2H_4O) **from Across Organics (99% purity)**. The ink **is** mixed and

milled by a roller to obtain a perfect uniform homogeneity. Initially polyvinyl butyral **is** dissolved in α-terpineol at 60°C with vigorous stirring for 30 minutes. The $Ba_{0.85}Sr_{0.15}TiO_3$ powder (previously dissolved in 2-(2-Butoxyethoxy) ethyl acetate) **is** added, **along with** polyethylene glycol to stabilize the mixture. **One hour after**, the ink of BST is heated at 100 °C for 1 hour to evaporate the solvent. Finally the ink **is submitted** to ultrasound and **passed** between the three-cylinder rollers in order to break the agglomerates. **The different BST85/15 ink preparation procedures are highly detailed in our earlier published work** [2]. The elaborated BST ink **is** deposited by screen printing on Pt/Ti/SiO2/Si substrates, the Pt (200nm **thick**) film serves as the bottom electrode **for our** capacitor **which are then** sintered for 1 **hour** at 100 °C. This operation was repeated for two times. Thereafter, the BST thick films were sintered in air for 2 h at 1100 °C to vaporize the organic compounds from the ink. Finally, to take electric measurements on the thick films, circular gold (**top** electrodes) with various diameters (0.1mm ~ 1mm) are deposited by thermal evaporation to obtain **Metal-Ferroelectric-Metal (MFM)** Au/BST/Pt capacitor structure. Fig. 1 shows the final structure of **this kind of capacitor.**

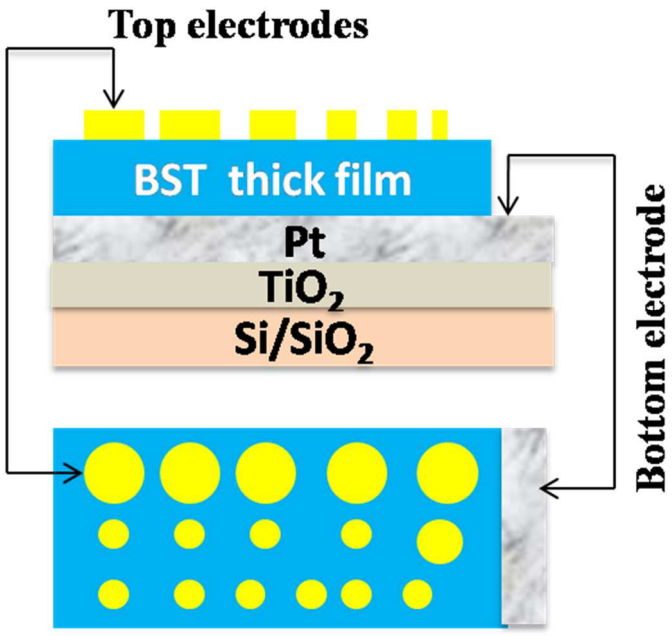

Fig. 1.

2.2 Characterizations techniques

The microstructure and the morphology of the prepared thick films were analysed by Xray diffraction **with a Philips X-ray diffractometer (model PW1710) using CuKα1 radiation (λ = 1,5406 Å)** and scanning Electron Microscopy **with a JEOLSEM (model JSM-5400)**. The dielectric measurements **are** carried out over a temperature range from room temperature (RT =25°C) up to 300°C and over a large frequency range (10^{-1} to 10^{6} Hz) using a temperature regulator (Linkam TMS94) and an impedance analyzer (Solartron 1260 coupled to a dielectric interface 1296). Capacitance-Voltage (C-V) measurements on the Au/BST(thick film)/Pt capacitor **are** studied using an Agilent LCR meter E4980A. The hysteresis characteristics **are** analyzed by a modified Sawyer Tower circuit at 10 kHz. The leakage currents characterizations (J-V) **are** recorded using a Keithley electrometer 6517A **in order to** identify the conduction mechanisms involved in these structures.

3. Results and discussion

3.1 Structural and morphological characterization

Fig. 2 **presents** the XRD patterns for the BST thick film. It can be observed from the graph the existence of different diffraction peaks of BST in the (10°-60°) 2θ range they are characteristics of BST (JCPDS File no. 39–1395) in this 2θ range. In addition, the calculated a-axis and c-axis lattice values are 3.9942 Å and 4.0171 Å, respectively. This suggests that the film is crystallized with the tetragonal structure phase at room temperature. The small Pt (111) phase detected in $2\theta \approx 40°$ is associated with the platinum bottom electrode.

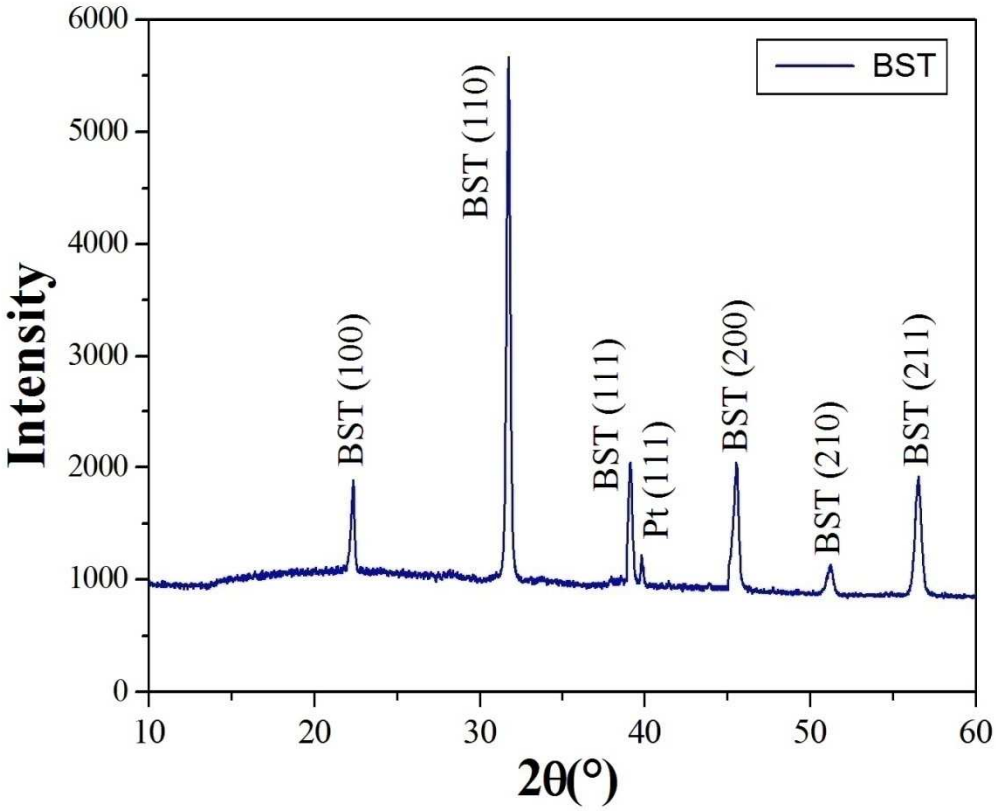

Fig. 2.

Fig. 3a and 3b exhibit the surface and the cross-section vision **of** the BST thick film, respectively. It is clear that a no cracks on the BST thick film **are** observed. The cross-section images show a generally uniform thickness of about ~20µm and an excellent adhesion to the Pt/Ti/SiO_2/Si substrate. The average gain size was measured to be 0.4 µm.

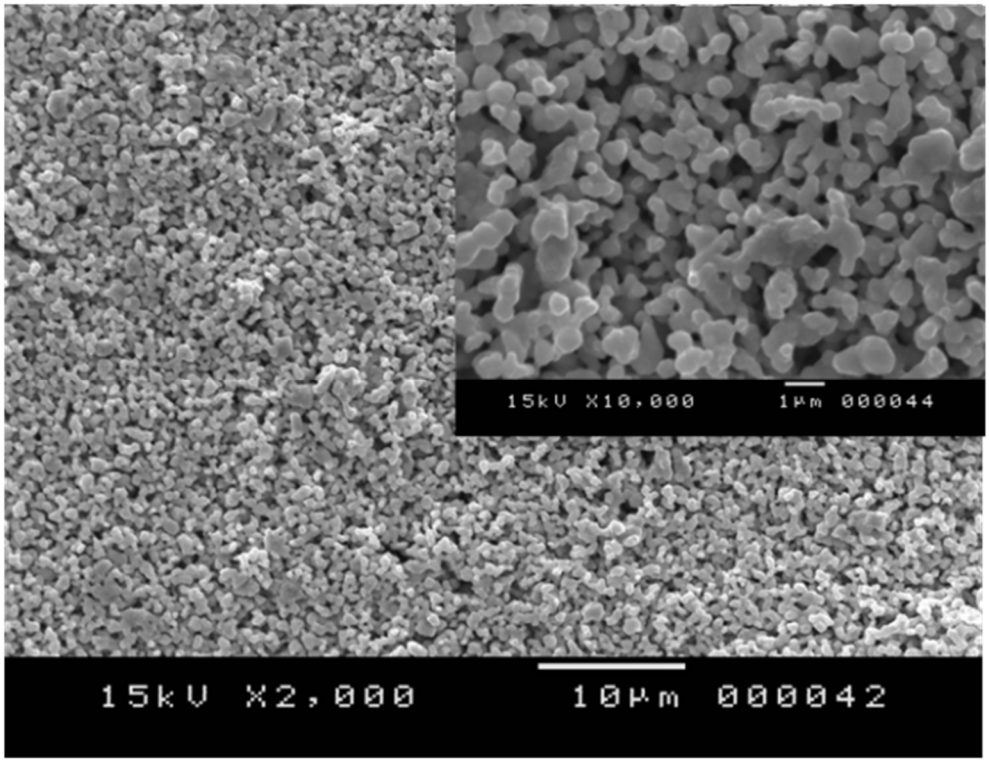
15kV X10,000 1μm 000044
15kV X2,000 10μm 000042

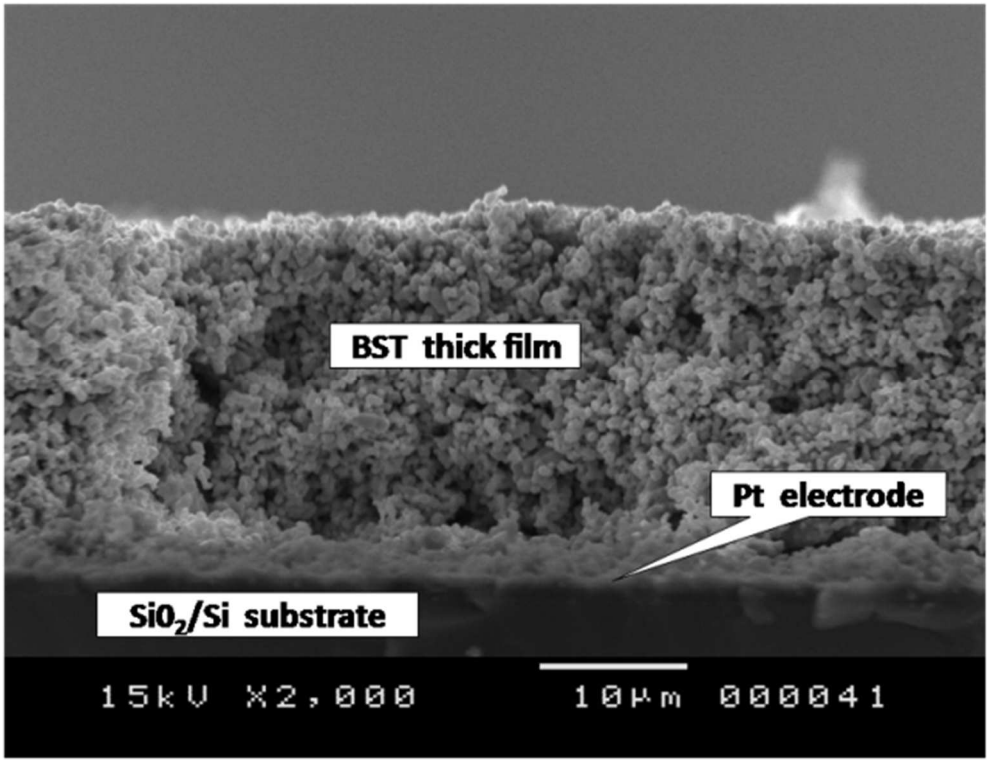
BST thick film
Pt electrode
SiO2/Si substrate
15kV X2,000 10μm 000041

Fig. 3.

3.2 Dielectric Analysis

3.2.1. Permittivity and loss studies

Dielectric measurements of BST thick film **are** studied as a function of **frequency** (10^{-1} Hz to 10^{6} Hz) and temperature (25°C-300°C). The variation of dielectric permittivity (ε'_r) is shown in Fig. 4.a. It's clear that for all temperature**s**, the ε'_r decrease **greatly** in the low-frequency and then **is** more or less **constant** at high frequency (F>500Hz) **which** constitute a dielectric dispersion phenomena. This behavior is a common feature for ferroelectric oxides materials [17] and can be due to the Maxwell-Wagner polarization [18, 19]. It is interesting to note that the elaborated BST 85/15 thick films show a high dielectric permittivity compared to BST 85/15 thick films deposited on alumina substrates by screen-printing process [2] **and compared to** BST 85/15 thin films deposited by sol-gel on Pt/Ti/SiO2/Si substrates published in our earlier work [20]. The frequency dependence of **the** dielectric loss factor ($tg(\delta)= \varepsilon''/\varepsilon'$) is also measured in the same **ranges of temperature and frequency and presented** in Figure 4b. The dielectric loss decrease with frequency displaying dispersion behavior due to Maxwell–Wagner interfacial polarization. The observed peak in $tg(\delta)$ confirms the existence of a dielectric relaxation in **our** BST **films** and also **signifies** that the hopping of charge carriers plays an important role in **the** transport mechanism [21] .

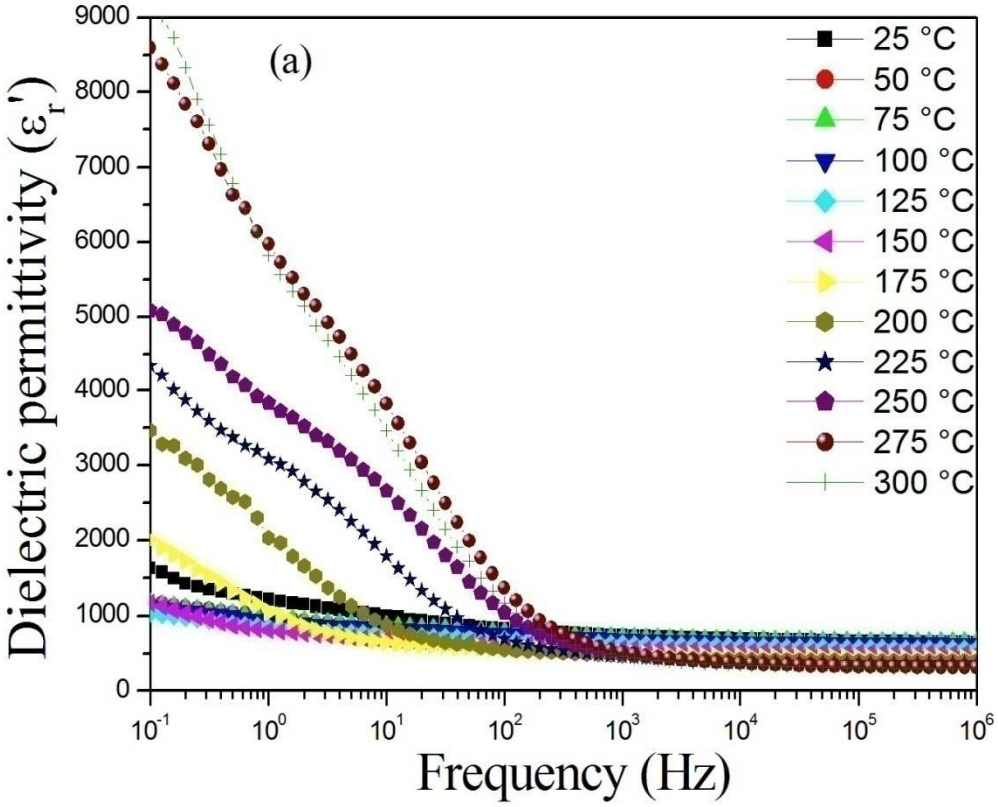
(a)
Dielectric permittivity (ε_r')
Frequency (Hz)
25 °C
50 °C
75 °C
100 °C
125 °C
150 °C
175 °C
200 °C
225 °C
250 °C
275 °C
300 °C
9000
8000
7000
6000
5000
4000
3000
2000
1000
0
10^{-1}
10^{0}
10^{1}
10^{2}
10^{3}
10^{4}
10^{5}
10^{6}

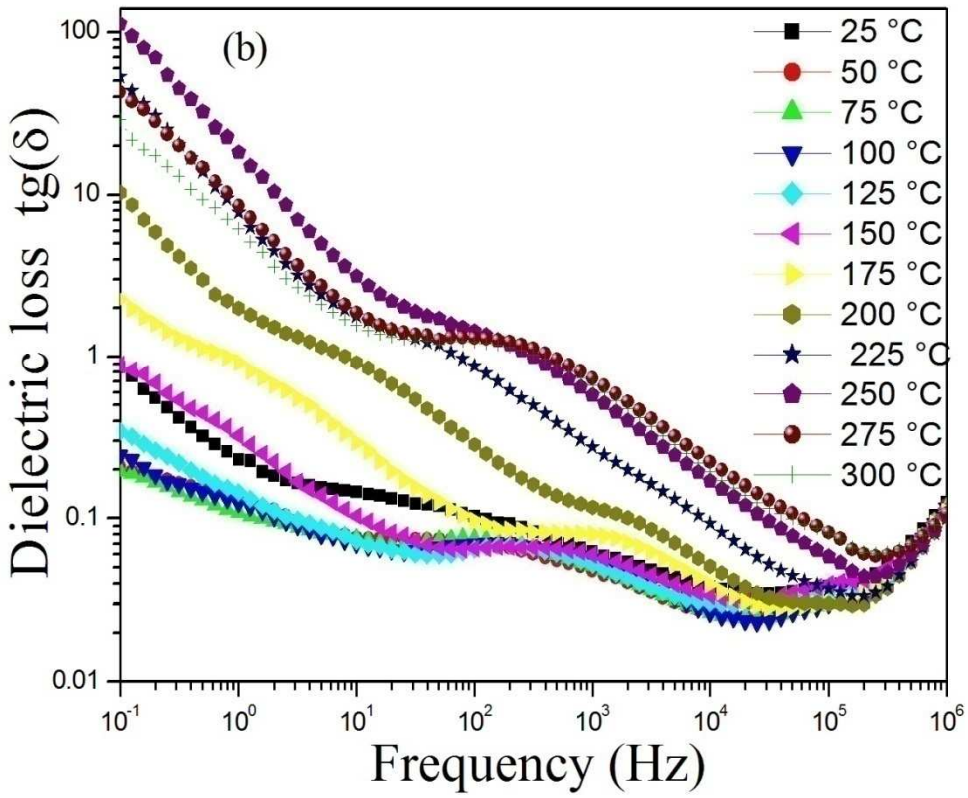

Fig. 4.

The variation of **εr'** of BST thick film with temperature for selected frequencies is **presented** in the Fig. 5a. The curve shows two maxima in the dielectric permittivity. The first peak is at 75°C = T_c **the Curie temperature** which corresponds to a ferroelectric–paraelectric phase transition in the BST system and the second peak **is** observed clearly at high temperatures **around** 270°C for low frequencies **under 10 kHz**. The appearance of second peak at high temperatures in **εr'** curves **as a function of temperature** is similar to that found in our earlier published work on sol-gel BST thin films [20], this behavior can be associated to the existence of nano/micropolar phases in the BST films **in the paraelectric state**. The obtained T_c value is different from **some of the ones** published on BST thick films deposited by screen printing process, for example X. Zhang et all; T_c = -2°C for BST 60/40 [14], X. U. Qing et all; T_c = 10°C for BST 60/40 [13] and B. Su et all; T_c = -30°C, 2°C and 30°C for BST 50/50, BST 60/40 and BST 70/30 respectively [22]. This difference

is clearly related to a difference of composition **since the temperature** T_C is very sensitive to the Sr and Ba ratio and **is** possibly associated to the substrate effect. The value of T_C found on our BST (85/15) thick films show that the material is in ferroelectric state at **room temperature**. This result is encouraging for several applications **such as** random access memories (RAM), radio-frequency identification (RFID) and ferroelectric capacitors, etc...

The variation of **dielectric loss tan(δ)** depending on the temperature for different frequency (Fig. 5b) present low values **inferior to** 0.05 in a large temperature range, ranging from **25** °C to 170°C. Above 170 °C the dielectric **loss** exhibits a remarkable increase, mainly due to the motion of oxygen vacancies. In fact, oxygen vacancies are thermally activated and become more mobile which increases**ing** the polarization [2]. The high values of the dielectric permittivity combined with the low loss values obtained **in** a wide temperature range makes the $Ba_{0.85}Sr_{0.15}TiO_3$ thick films **a potential** candidates for many modern microelectronic applications.

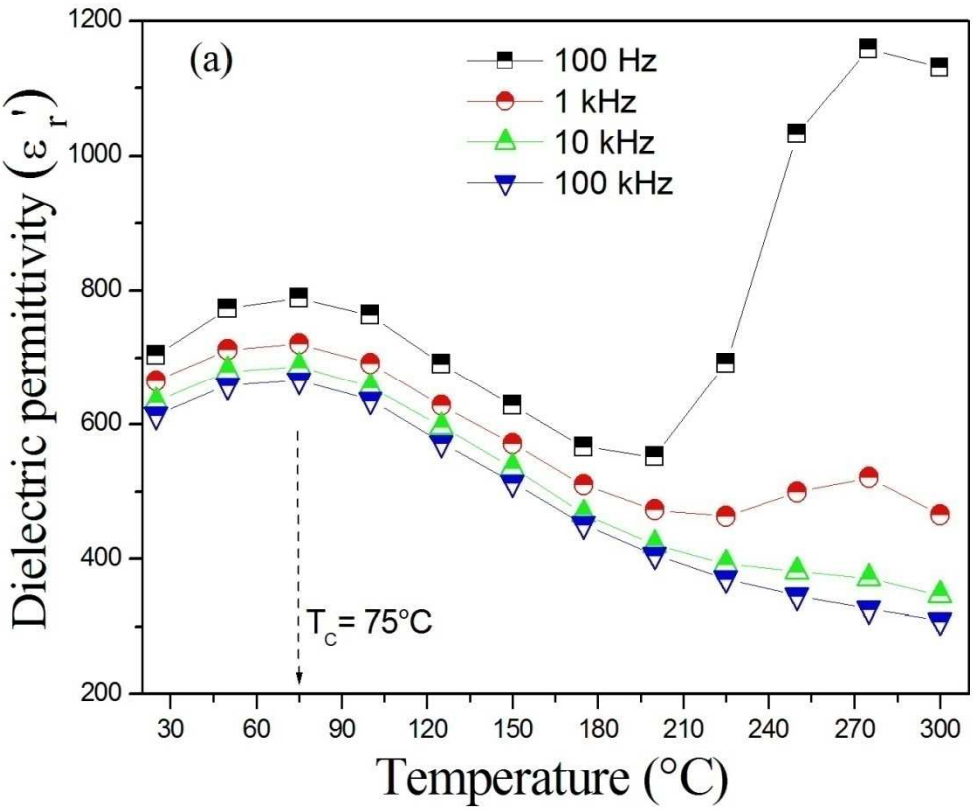

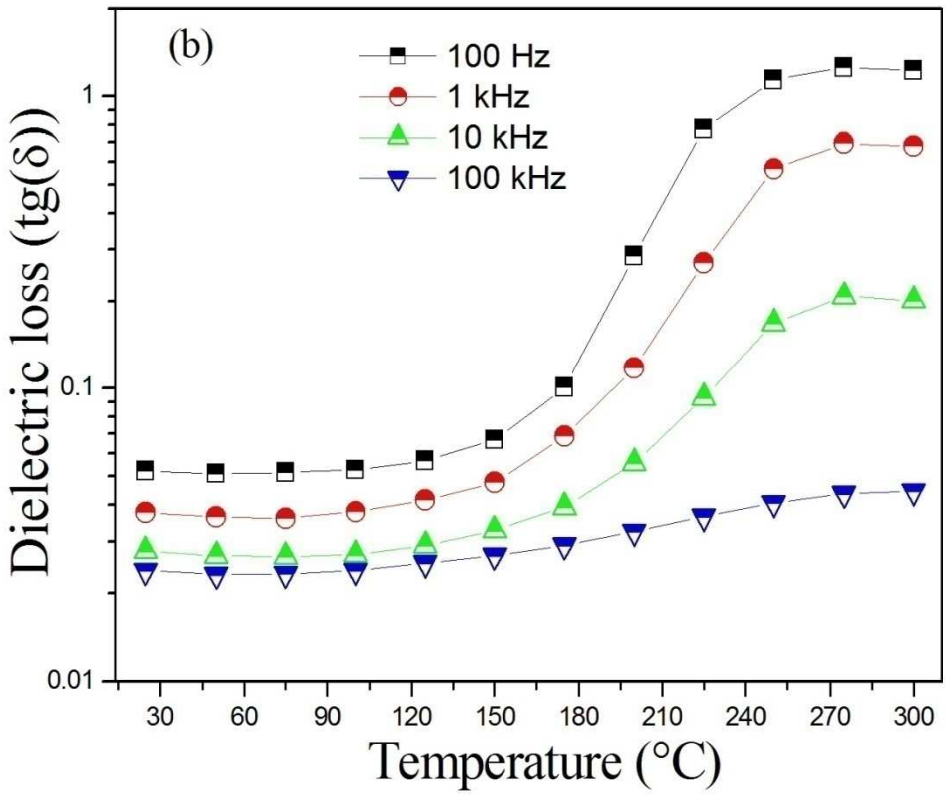

Fig. 5.

3.2.2. AC Conductivity Analysis

Using the **ε'r** and tan (δ) measurements, the ac electrical conductivity (σ_{ac}) of our BST thick films can be **determined** from the empirical expression: $\sigma_{ac} = \omega\, \varepsilon' \varepsilon_0 \tan(\delta)$, Where ω is the angular frequency and ε_0 is the vacuum permittivity. Fig. 6 presents the frequency dependence of σ_{ac} at various temperatures (150°C-300°C). **On this graph we** can observe two regions, at low frequen**cies**; the conductivity is practically **constant** with frequency **which** corresponds to the dc bulk conductivity (σ_{dc}). But **while** in the high frequen**cies** region, the σ_{ac} varies greatly with frequency. Therefore the ac conductivity can be investigated by Jonscher's power law equation:

$$\sigma_{ac} = \sigma_{dc} + A\omega^{n} \qquad (1)$$

Where, A is a pre-exponential constant, and n is the power-law exponent [23]. It is clear from figure that the σ_{dc} conduction process is thermally activated, so σ_{dc} can be obeys the Arrhenius law:

$$\sigma_{dc} = \sigma_0 \, e^{\left[\frac{-E_\sigma}{K_B T}\right]} \qquad (2)$$

Where k_B is the Boltzmann constant, T is the temperature in Kelvin, σ_0 is the pre-exponential factor, and E_σ is the dc conductivity activation energy. We **have drawn** σ_{dc} versus 1000/T at **0.1 Hz in the inset of Fig.6**. The obtained **E_σ** value is about **1.06 ±0.05eV** which can be **attributed to** the migration of oxygen vacancies in BST [21]. **This value is of the same order of magnitude as we published for thin BST85/15 films from 200 to 400 nm thick deposited on Pt/Ti/SiO2/Si substrates** [20].

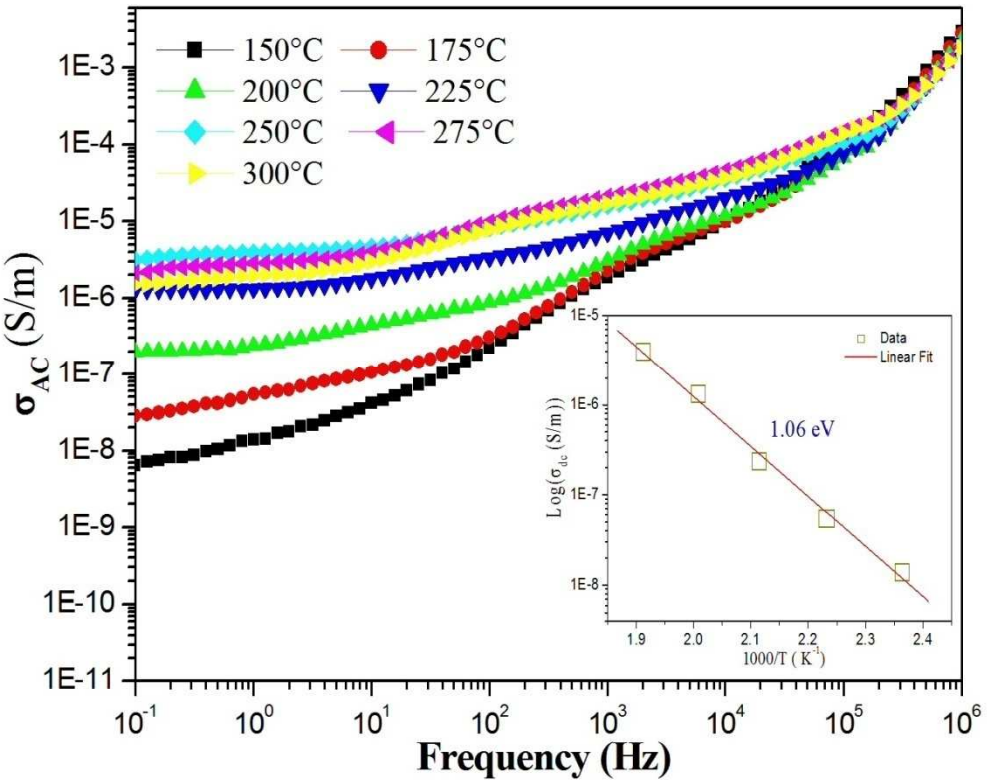

Fig. 6.

3.3. Tunability and hysteresis behavior

Fig. 7a illustrates the C–V curves obtained at room temperature at 10 kHz from -20 to +20V. The appearance of **a** butterfly form in the curves and the strongly nonlinear voltage confirm the good ferroelectric characteristics of the BST thick film occurring from domain switching. The dielectric tunability is defined by the following expression [24, 25]:

$$\eta_r = (1 - \frac{C_{min}}{C_{max}}) \times 100 \qquad (3)$$

As shown in Fig.7a, C_{max} is the maximum value of the capacitance which in our case is about 275pf either at+5Vor at-5Vand C_{min} is the minimum value of the capacitance, which in our case is about 50pf either at +20 V or at -20 V. The tunability at 20 Volts is about 81%, this value is higher than a recent published one on BST thick film of the same composition and same preparation technique deposited on alumina substrate [2]. To the best of our knowledge, the value of 81% is the uppermost reported for a BaSrTiO3 in different **forms of films (thin / thick) and in ceramics**. **A comparison with published tunability in the literature is given in the following table.**

Table 1.

Composition	Form	Tunability @ Electric field	References
BST (85/15)	Thick film	81% @ 10kV/cm	This work
BST (85/15)	Thick film	67% @ 60kV/cm	[2]
BST (70/30)	Ceramic	69% @ 17kV/cm	[8]
BST (70/30)	Thin film	42% @ 600kV/cm	[8]
BST (60/40)	Ceramic	40% @ 66kV/cm	[13]
BST (70/30)	Thick film	43% @ 66kV/cm	[13]
BST (70/30)	Thick film	29% @ 66kV/cm	[13]
BST(60/40)	Thick film	60% @ 57kV/cm	[14]
BST (90/10)	Thin film	30% @ 125kV/cm	[24]

Our obtained tunability of 81% corresponds to an increase by a factor **of 5.3** of the capacitance (and therefore of the **dielectric** permittivity). Such a variation can be well compared to the one of a tunable varactor diode and is very attractive for tunable microwaves applications such as filters, antenna beam steering, and tunable capacitor **as well as for tunable optical applications such as refractive index, filters and MEMS. The evolution of the tenability as a function of the electric field is given in** Fig. 7c**. The tenability curve is not symmetrical which can be attributed to the different nature of**

the used electrodes (Au and Pt). The ferroelectric hysteresis loop of the Au/BST (thick film)/Pt **is** measured at room temperature at 10 kHz (Fig. 7b). The existence of a remnant polarization confirms that our film is in a ferroelectric phase. **Moreover, the** remanant polarization (P_r) value is estimated to be 5µC/cm^2. This result is **almost ten times better than** those for screen printed BST thick film deposited on alumina substrate Pr = 0.57 µC/cm^2 reported by X.-F. Zhang et al [14]. **Then**, the remanent polarization of 5 µC/cm² is encouraging for FeRAM technology [26]. **It can be also observed that the saturation polarization is P_{sat}=8µC/cm^{2}and the coercive voltage is E_C= 5 V which corresponds to an electric field of 2.5 kV/cm. This low voltage value allows to switch a ferroelectric domain corresponding to a bit in a FeRAM.**

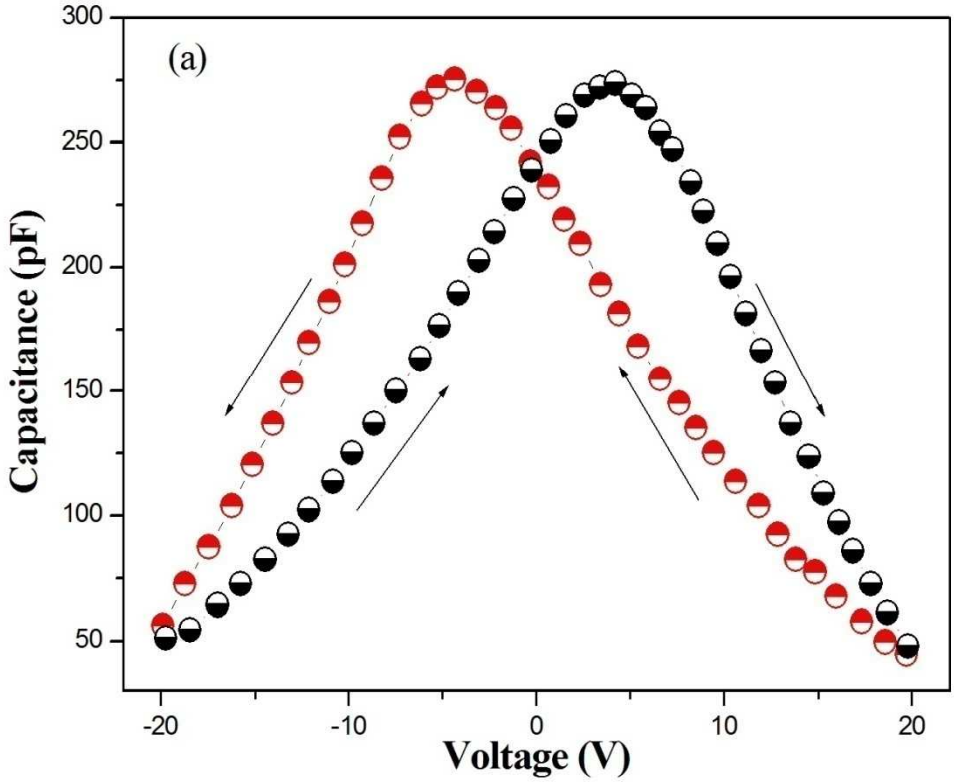
(a)
Capacitance (pF)
300
250
200
150
100
50
-20
-10
0
10
20
Voltage (V)

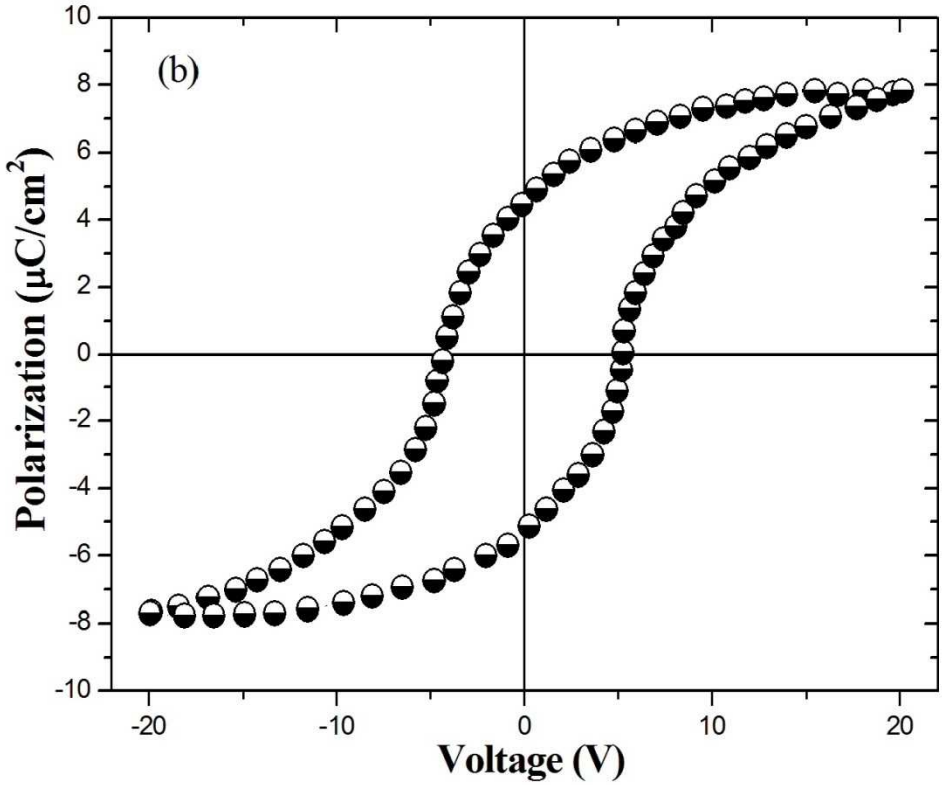
(b)
Polarization (μC/cm²)
Voltage (V)
10
8
6
4
2
0
-2
-4
-6
-8
-10
-20
-10
0
10
20

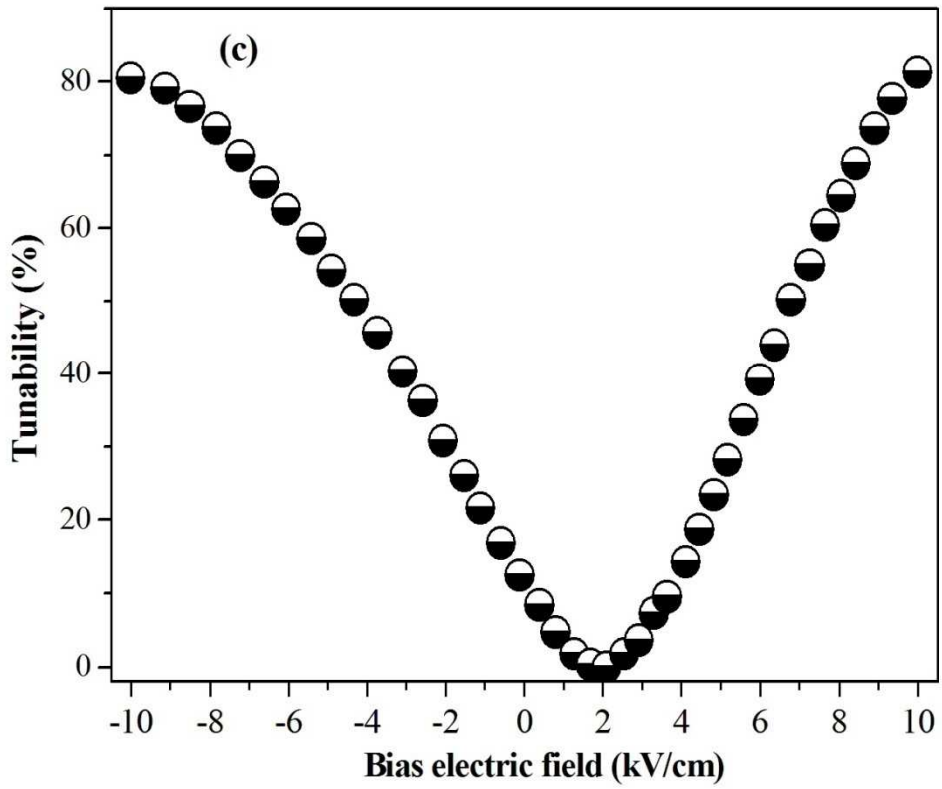
(c)
Tunability (%)
80
60
40
20
0
-10
-8
-6
-4
-2
0
2
4
6
8
10
Bias electric field (kV/cm)

Fig. 7.

3.4. Leakage current measurements

Fig. 8a display the leakage current density of BST capacitor as a function of applied voltage in the (-20V − +20V) range. The leakage current density (J) is smaller than 10^{-5} A/cm^2 in the whole voltage range. The leakage current density curves are not symmetrical which can be attributed to the different nature of the used electrodes (Au and Pt). The J-V behavior reveals that various leakage mechanisms **occurring** in the negative and positive bias region. Generally, the **conduction process can be governed by several mechanisms**, including Poole frenkel effect, Schottky emission, Ohm's law and SCLC emission [9, 21, 27].These different mechanisms **can either contribute simultaneously or one of them playing the dominant role in the conduction**. To investigate the conduction mechanism in our $Ba_{0.85}Sr_{0.15}TiO_3$ **films** in positive applied voltage, the leakage current density (J) is **plotted** against **applied voltage (V) in a log(J) versus log(V) graph as shown** in Fig. 8b. It can be **clearly observed** that there are two separate regions. For low voltages, the log(J) versus log(V) curve has slope of 1.11, which is value very close to 1, indicating that Ohm's law plays a major role in the conduction mechanism in this voltage region [28]. At high voltage, **the curve** reveals a slope close to 2, which is in **a** good agreement with (SCLC) **model** [29]. For high voltages i.e. high electric field, with a negatively biased Au electrode, the Schottky model can be employed to study the leakage current measurement. The current density J is then given by [30].

$$J = A^{**}T^2 \; e^{\left(-\frac{q\varphi_B}{KT}\right)} \times e^{\left(\frac{q}{KT}\sqrt{\frac{qE}{4\pi\varepsilon_0\varepsilon}}\right)} \qquad (4)$$

Where A**, E, ϕ_B, q, ε_0, ε, k , are **respectively** the effective Richardson constant, **the** applied electric field, **the** Schottky barrier height at the Au electrode, **the** electronic charge, **the dielectric permittivity of the** free space, **the optical** dielectric constant and the Boltzmann constant, respectively. If the conduction mechanism at high electric field is related to Schottky emission, the log J versus $\sqrt{E}$ plot **should** to be a straight line and the slope **would** provide the optical dielectric constant of BST. **We found in Fig.8c a value of 3.55 which is in accordance** with the square of the refractive index n [28, 31].

In Fig. 8c, log J is traced as a function of $\sqrt{E}$. It's clear that for applied electric field higher than a threshold value, the Schottky equation provides a good fit with the leakage current curve, as presented by the solid line **in Fig. 8c**. **The value 3.55 is comparable to** the known optical dielectric constant value of about 4. So, at a high negative voltage, the leakage current of BST thick films can be well described by the Schottky equation.

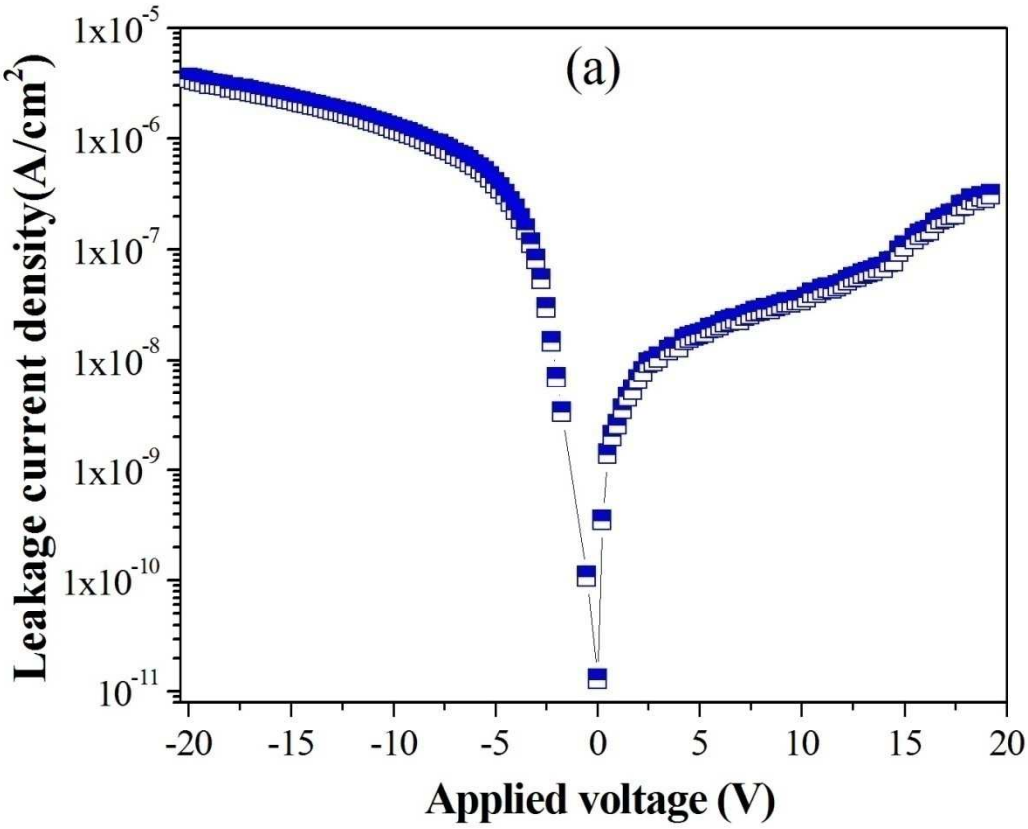

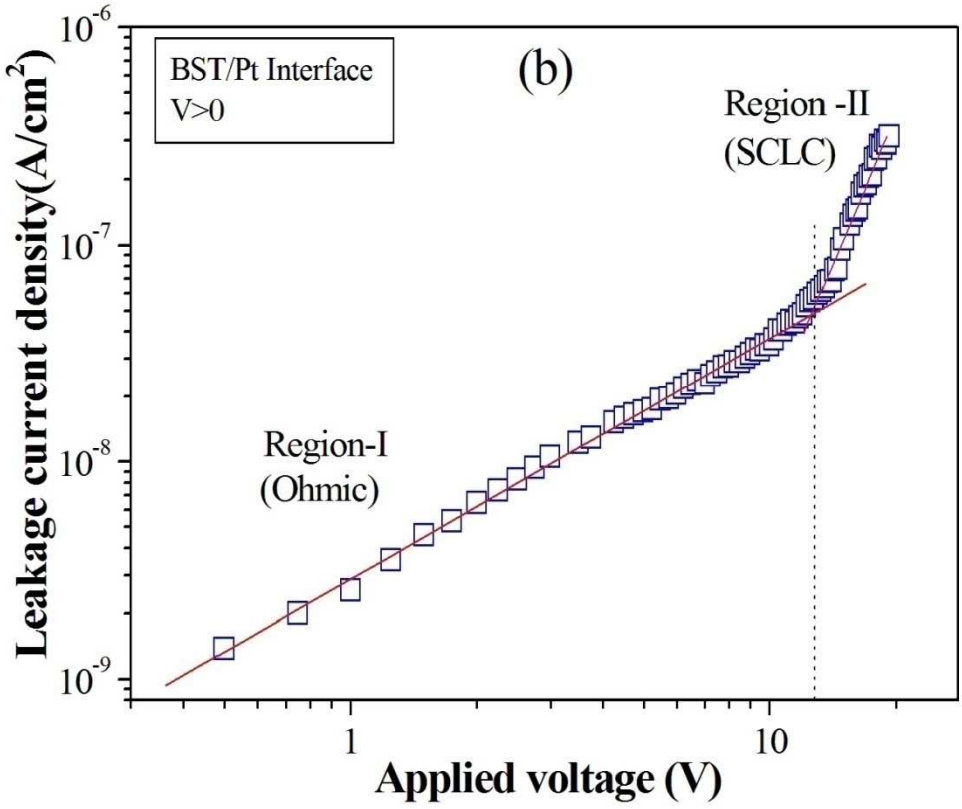
BST/Pt Interface
V>0
(b)
Region -II
(SCLC)
Region-I
(Ohmic)
Leakage current density(A/cm^2)
Applied voltage (V)
10^{-6}
10^{-7}
10^{-8}
10^{-9}
1
10

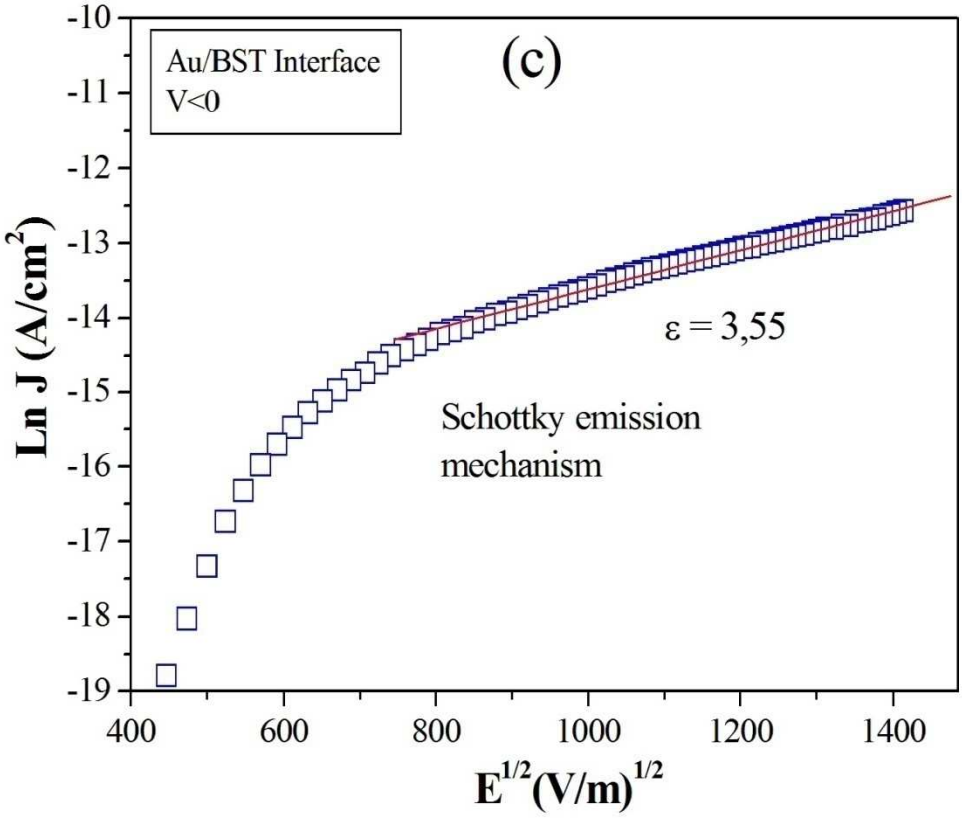

Fig.8

4. Conclusions

In this work, high-quality Ba0.85Sr0.15TiO3thick films (20µm) are successfully fabricated by screen-printing technique on Pt/Ti/SiO2/Si substrates. AC and DC measurements are carried out. The temperature dependence of the dielectric constant shows two peaks: the first one appears at 75°C and is attributed to the ferroelectric-paraelectric transition (Curie temperature), while the origin of the second peak observed at high temperature (270 °C) and low frequency can be related to the existence of nano/micropolar phases in the BST films. The leakage current in Au/ BST/Pt capacitor reveals an asymmetric behavior at positive and negative bias. At a high electric field, in the positive bias region the leakage current shows SCLC behavior. In the negative bias region, the leakage current is dominated by Schottky emission. The

high values of the dielectric permittivity combined with low values of the dielectric loss and leakage currents show high performance of our Au/$Ba_{0.85}Sr_{0.15}TiO_3$/Pt capacitors. This structure is very encouraging in the areas of thick film technology and presents a substitute for Pb-based materials Moreover , the high tunability (81%) makes $Ba_{0.85}Sr_{0.15}TiO_3$ thick films a potential candidate for functional applications like tunable varactor diode and tunable capacitor devices.

References:

[1] A.I. Khan, A. Keshavarzi and S. Datta , The future of ferroelectric field-effect transistor technology, Nature Electronics 3 (2020) 588–597

[2] A. Selmi, M. Mascot, F. Jomni, and J.-C.Carru' High tunability in lead-free Ba0.85Sr0.15TiO3 thick films for microwave tunable applications. Ceramics International. B 45 (2019) 22445-23856.

[3] S. Said, M. Sabri, and F. Salleh, Ferroelectrics and Their Applications, (2017) doi:10.1016/B978-0-12-803581-8.04143-6

[4] Y. Slimani, B. Unal, M. A. Almessiere, E. Hannachi, Ghulam Yasin, A. Baykal , I. Ercan , Role of WO3 nanoparticles in electrical and dielectric properties of BaTiO3– SrTiO3 ceramics Journal of Materials Science: Materials in Electronics 31 (2020) 7786–7797.

[5] Y. Slimani, B. Unal, E. Hannachi, A. Selmi, M.A. Almessiere, M. Nawaz, A. Baykal, I. Ercan, M. Yildiz, Frequency and dc bias voltage dependent dielectric properties and electrical conductivity of BaTiO3- SrTiO3/(SiO2)x nanocomposites, Ceramics International 45 (2019) 11989-12000

[6] E. Hannachi,Y. Slimani, F.Ben Azzouz, A. Ekicibil , Higher intra-granular and inter- granular performances of YBCO superconductor with TiO2 nano-sized particles addition, Ceramics International 44 (2018) 18836-18843.

[7] K. Seevakan, A. Manikandan, P. Devendran, Y. Slimani, A. Baykal, T. Alagesan, Structural, magnetic and electrochemical characterizations of Bi2Mo2O9 nanoparticle for supercapacitor application, Journal of Magnetism and Magnetic Materials 486 (2019) 165254;

[8] A. Ahmed, I. Goldthorpe, A.K. Khandani, Electrically tunable materials for microwave applications, Applied Physics Reviews 2 (2015) 011302.

[9] A. Selmi , M. Mascot , F. Jomni , J.-C. Carru ; Investigation of interfacial dead layers parameters in Au/ Ba0.85Sr0.15TiO3/Pt capacitor devices, Journal of Alloys and Compounds 826 (2020) 154048

[10] D. Fasquelle, M. Mascot, N. Sama, D. Remiens, J.-C. Carru, Lead-free piezoelectric thin films for RoHS devices, Sensors and Actuators A 229 (2015) 30–35

[11] P. Kumari , R. Rai , S. Sharma , M. Shandilya , and Ashutosh Tiwari, State-of-the-art of lead free ferroelectrics: A critical review, Adv. Mater. Lett, 6, (2015) 453-484

[12] H. Yuan, J. Liu , M. Gu, S. Feng, M. Zhou, Y. Luo, Low-temperature sintering and electrical properties of Ba0.68Sr0.32TiO3 thick films , Ceramics International, (2021) https://doi.org/10.1016/j.ceramint.2021.02.235

[13] Q. Xu, D. Zhan, D.P. Huang, H.X. Liu, W. Chen, F. Zhang, Effect of oxygen-ion motion on dielectric properties of $Ba_{0.6}Sr_{0.4}TiO_3$ thick films, Materials Research Bulletin 70 (2015) 99-105.

[14] X-F. Zhang, Q. Xu, D. Zhan, H-X. Liu, W. Chen, D-P. Huang, Dielectric evaluation of electrically tunable $Ba_{0.6}Sr_{0.4}TiO_3$ thick films prepared by screen printing, Ceram. Int.38 (2012) 3465-3472.

[15] B. Su, T.W. Button, Interactions between barium strontium titanate (BST) thick films and alumina substrates, Journal ofthe European Ceramic Society 21 (2001) 2777–2781

[16] F. Xiang, H. Wang, M. Zhang, X. Sun, X. Yao, Preparation and dielectric tunability of bismuth-based pyrochlore dielectric thick films on alumina substrates, Ceram. Int. 34 (2008) 925-928.

[17] Y. Slimani, A. Selmi, E. Hannachi, M.A. Almessiere, M. Mumtaz, A. Baykal, and I. Ercan, Study of tungsten oxide effect on the performance of $BaTiO_3$ ceramics, J. Mater. Sci.: Mater. Electron. 30 (2019) 13509-13518.

[18] Y. Slimani, A. Selmi, E. Hannachi, M.A. Almessiere, A. Baykal, and I. Ercan, Impact of ZnO addition on structural, morphological, optical and electrical performances of $BaTiO_3$ ceramics, J. Mater. Sci.: Mater. Electron. 30 (2019) 9520-9530.

[19] A. Selmi, A. Fkiri, J. Bouslimi, H. Besbes, Improvement of dielectric properties of ZnO nanoparticles by Cu doping for tunable microwave devices, J Mater Sci: Mater Electron 31 (2020)18664–18672.

[20] A. Selmi, O. Khaldi, M. Mascot, F. Jomni J.-C. Carru, Dielectric relaxations in $Ba_{0.85}Sr_{0.15}TiO_3$ thin films deposited on $Pt/Ti/SiO_2/Si$ substrates by sol–gel method, J. Mater. Sci.: Mater. Electron. 27 (2016) 11299-11307.

[21] O. Khaldi , F. Jomni , P. Gonon , C. Mannequin , B. Yangui, Investigation of electrical properties of HfO2 metal–insulator–metal (MIM) devices, Applied Physics A , 116, (2014) 1647–1653

[22] B. Su, J.E. Holmes, C. Meggs, T.W. Button, Dielectric and microwave properties of barium strontium titanate (BST) thick films on alumina substrates, Journal of the European Ceramic Society 23 (2003) 2699–2703

[23] A. K. Jonscher, The 'universal' dielectric response, Nature 267 (1977) 673-679.

[24] D. Fasquelle, M. Mascot, J.C. Carru, Electrical properties optimization of Ba0.9Sr0.1TiO3 thin films deposited by sol-gel, Advanced Materials Research 277 (2011) 1-10

[25] V. Eswaramoorthi, and R. V. Williams, Effect of thickness on microstructure, dielectric and dptical properties of single layer Ba0.6Sr0.4TiO3 thin Film, Surface Review and Letters, 21 (2014) 1450020-1450028

[26] R.E. Jones, Jr., P. Zurcher, P. Chu, D.J. Taylor, Y.T. Lii, B. Jiang, P.D. Maniar, and S.J. Gillespie, Memory applications based on ferroelectric and high-permittivity dielectric thin films, Microelectronic Engineering 29 (1995) 3-10

[27] L. Pintilie , I. Vrejoiu, D. Hesse, G. LeRhun, and M. Alexe, Ferroelectric polarization-leakage current relation in high quality epitaxial Pb,,Zr,Ti…O3 films, PHYSICAL REVIEW B 75 (2007) 104103

[28] S.Y. Wang, B.L. Cheng, C. Wang, W. Peng, S.Y. Dai, Z.H. Chen, Dielectric and Ferroelectric Properties of Ba1-xSrxTiO3 Thin Films Prepared by Pulsed Laser Deposition, Key Engineering Materials 280 (2005) 81-84.

[29] K. Tao, Z. Hao, B. Xu, B. Chen, J. Miao, H. Yang, B.R. Zhao, Ferroelectric properties of (Ba,Sr)TiO3 thin films grown on YBa2Cu3O7 layers J. Appl. Phys. **94** (2003) 4042

[30] N.T.M. Pham, A.B. Boukamp, M.J.H. Bouwmeester, A.H.D. Blank, Microstructural and electrical properties of nanocomposite PZT/Pt thin films made by pulsed laser deposition, Ceram. Int. 30 (2004) 1499–1503.

[31] S. Zafar, R.E. Jones, B. Jiang, B. White, V. Kaushik, S. Gillespie, The electronic conduction mechanism in barium strontium titanate thin films, Appl.Phys. Lett. 73 (1998) 3533-3535.

List of Tables :

Table 1. A comparison with published tunability of $Ba_{1-x}Sr_xTiO_3$ in the literature.

List of Figures :